A DOSIMETRIC DATABASE AND CORRELATION STUDY FOR PROTON-INDUCED SECONDARY PARTICLES

by

Nursel SAFAKATTI KARAKOC [1], Hiroshi WATABE [2], Peter Kwan Ngok YU [3], Dragana Ž. KRSTIĆ [4], Dragoslav R. NIKEZIĆ [4], Zoran M. JOVANOVIĆ [5], Abul Kalam Fazlul HAQUE [6], Rafiqul ISLAM [7], and Mehrdad SHAHMOHAMMADI BENI [2,3*]

[1] Graduate School of Biomedical Engineering, Tohoku University, Sendai, Japan
[2] Division of Radiation Protection and Nuclear Safety,
Research Center for Accelerator and Radioisotope Science, Tohoku University, Sendai, Japan
[3] Department of Physics, City University of Hong Kong, Hong Kong, China
[4] Faculty of Science, University of Kragujevac, Kragujevac, Serbia
[5] Department of Natural Science and Mathematics, State University of Novi Pazar, Novi Pazar, Serbia
[6] Atomic and Molecular Physics Laboratory, Department of Physics, University of Rajshahi, Rajshahi, Bangladesh
[7] Institute of Nuclear Medical Physics AERE, Bangladesh Atomic Energy Commission, Dhaka, Bangladesh

Scientific paper
https://doi.org/10.2298/NTRP2503175S

In response to the high demand for proton therapy as a cancer treatment method in recent years, comprehensive studies have been conducted to improve the accuracy of dose calculations. However, the secondary particles produced during proton irradiation at energies 70-250 MeV present significant challenges, as they may induce radiation-related damage in surrounding non-target tissues and materials. To address these issues, we developed an open-source database and computer program named Proton-induced Secondary Emission Database, ProtonSED. The present database incorporates National Institute of Standards and Technology compounds and elements in a unit-volume cylinder to determine the primary protons and secondary particles such as neutrons, photons, and alpha particles. The correlation matrices for energy deposition from primary protons and secondary particles were also determined. The present database and correlation matrix approach will be useful for irradiation involving high-energy proton beams.

Key words: particle and heavy ion transport code system, Monte Carlo method, proton therapy, secondary emission database

INTRODUCTION

Among the various techniques used to combat cancer, proton therapy has emerged as particularly promising due to its unique characteristic of delivering a well-defined range within the target medium [1-3]. While this well-defined range is crucial for accurately localizing the dose to the tumor, the sharp energy deposition of the Bragg peak is even more decisive in delivering the therapeutic effect within the target tissue. Incident proton beams are commonly used in therapeutic setups and have incident energy in the range of 70-250 MeV. These proton beams are produced using either cyclotrons or synchrotrons [4]. Within the 70-250 MeV energy range, the generation of secondary particles-including photons, neutrons, and alpha particles-is highly probable, with the production rates governed by the nuclear and physical properties of the target material [5,6]. The emitted secondary particles can deposit dose along their tracks, thereby altering the overall dose distribution and potentially introducing unintended biological side effects. Previous Monte Carlo (MC) studies have addressed scattered radiation fields in X-ray diagnosis, benchmarking of photon- beam simulation toolkits, and dosimetry of brachy- therapy sources [7-9], underscoring the need to specifically quantify secondary radiation from therapeutic proton beams in different media. Previously, Jiang *et al*. [10] used the GEANT4 MC package to determine the secondary doses in proton therapy and demonstrated that secondary neutrons significantly contributed to the overall effective dose deposition in non-targeted organs. Moreover, the neutron energy spectrum generated by the 250 MeV incident proton beam was experimentally determined and later validated by employing MC computations [11], thereby confirming the importance of secondary particle production from proton beams. In addition to dose deposition, the secondary particles can induce various types of

* Corresponding authors, e-mail: ben.sh@tohoku.ac.jp

radiation-related damage in the target material. This damage is primarily due to their distinct patterns of energy deposition. Previous studies [12, 13] have shown that secondary particles, especially neutrons, increase the lifetime risk of developing secondary cancers in patients who have undergone proton therapy. Therefore, it is important to study the dose deposition from proton-induced secondary particles in commonly used materials in proton irradiation facilities. The most common approach to determining dose deposition from secondary particles is the use of MC methods to model the transport and interactions of ionizing radiation with matter. In this context, several well-established multi-purpose MC packages have been developed, including Monte Carlo N-Particle (MCNP) [14], Geant4 [15], FLUKA [16], and particle and heavy ion transport code system (PHITS) [17]. However, modelling of this multi-particle systems would be tedious, time-consuming, error-prone, and computationally expensive [18, 19]. Users must also familiarize themselves with well-established MC packages that require a license for access. This further complicates the task of studying secondary emissions because of proton irradiation. Given the importance of secondary particle generation by incident proton beams, some studies choose to overlook secondary emissions resulting from proton irradiation, which is not advisable. For example, Shan *et al*. [20] offered an approach to enhance dose calculation efficiency in proton therapy by avoiding the simulation of secondary particles. However, this approach could potentially undermine the accuracy of realistic dosimetry, as discussed earlier. The studies conducted by Ekinci *et al*. [21] examined initial proton beam characteristics within different biomaterials. However, it is essential to acknowledge that the secondary particle emissions resulting from proton beam induction have a significant effect on treatment safety and efficiency. Considering these challenges, we have developed an extensive secondary emission database for most elements and compounds reported in the NIST database [22] in the range of 70 MeV to 250 MeV incident proton beam impinging on a unit-volume cylinder. These were generated using the PHITS MC package and further verified using the MCNP package version 6.2. In addition, we developed a user-friendly graphical user interface (GUI) to facilitate data retrieval from the secondary emission database. Correlations between energy deposition from incident protons and secondary particles in different materials were investigated using a correlation matrix approach. We believe the database and correlation matrices will be useful for estimating the contribution of secondary particles to the deposited dose in proton irradiation.

MATERIALS AND METHODS

The main part of the present work is the code generator program that automatically builds scripts by looping through the NIST material library [22]. This generates a PHITS MC script for proton irradiation of a unit volume cylinder from 70 MeV to 250 MeV with 1 MeV intervals that adds up to a total of 181 irradiation scenarios for every material (elements and compounds). The program sets material definitions, densities, and respective tallies for primary protons and secondary particles (photons, neutrons, and alpha particles) in the modeled unit-volume cylinder. The schematic representation of the proton irradiation setup is shown in fig. 1. In the present database, a total of 48 compounds and 24 elements were taken from NIST material composition data [22] and summarized in tab. 1.

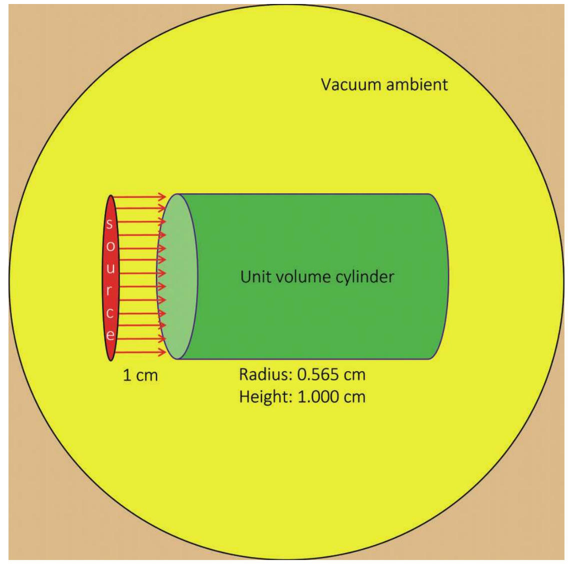

Figure 1. Schematic representation of the proton irradiation setup used in the ProtonSED, showing a unit volume cylinder and a proton disk source

The code generator program, developed to build the present database, automatically created specific directories for the materials listed in tab.1 and generated proton irradiation scripts.

The program automatically invokes the PHITS MC package to run these transport computations. Once the run is completed, the program extracts dosimetric data from the generated tally files and writes them into the database file. As in our previous works [23-26], the GUI was developed using the QT5 libraries and written entirely in the C++ programming language. On the other hand, the code generator program was written in the FORTRAN90 programming language. All components were compiled using the GCC compiler toolkit version 11.3.1-2. The GUI collects user input and forwards them to the program's data retrieval component. This component then retrieves the secondary emission data from the established database.

The Script button provides users with a sample script at 70 MeV incident proton energy for all elements and compounds. This feature is particularly useful for inspecting input scripts automatically prepared by the code generator program. The ProtonSED GUI is shown in fig. 2. The program offers a straightforward and easy-to-use interface to users.

Table 1. List of compounds and elements considered in the present database

Compounds	Elements
Tissue equivalent plastic	Hydrogen (H)
Acetylene	Helium (He)
Adipose tissue	Beryllium (Be)
Air	Carbon (C)
Al_2O_3	Nitrogen (N)
Bone equivalent plastic	Oxygen (O)
Bone compact	Sodium (Na)
Bone cortical	Aluminum (Al)
Air equivalent plastic	Silicon (Si)
CaF_2	Argon (Ar)
CO_2	Titanium (Ti)
Cellulose nitrate	Iron (Fe)
CsI	Copper (Cu)
Ethylene	Germanium (Ge)
Ferrous sulfate solution	Krypton (Kr)
Pyrex glass	Molybdenum (Mo)
Kapton polyimide	Silver (Ag)
LiF	Tin (Sn)
Lithium tetraborate	Xenon (Xe)
M3 wax	Gadolinium (Gd)
Methane	Tungsten (W)
MS20 tissue substitute	Gold (Au)
Muscle, skeletal	Lead (Pb)
Muscle, striated	Uranium (U)
Muscle equivalent liquid, with sucrose	
Muscle equivalent liquid, without sucrose	
Nylon type 6	
Paraffin wax	
Photographic emulsion	
Plastic scintillator	
Polycarbonate	
Polyethylene	
Mylar	
Polymethyl methacrylate	
Polypropylene	
Polystyrene	
Teflon	
Polyvinyl chloride	
Propane	
SiO_2	
NaI	
Stilbene	
Tissue equivalent gas, methane	
Tissue equivalent gas, propane	
Toluene	
Water, liquid	
Water, vapor	

Considering the large amount of data in the database, we selected a subset of elements and compounds for validation and verification using the PHITS and MCNP6.2 MC packages. Since the database was generated using the automatic code generator routine, it was pertinent to manually run several cases with PHITS to ensure the accuracy of the reported results. Moreover, comparison with MCNP6.2 further contributed to the validation of our model. The selected elements and compounds at specific incident proton beam energies are listed in tab. 2.

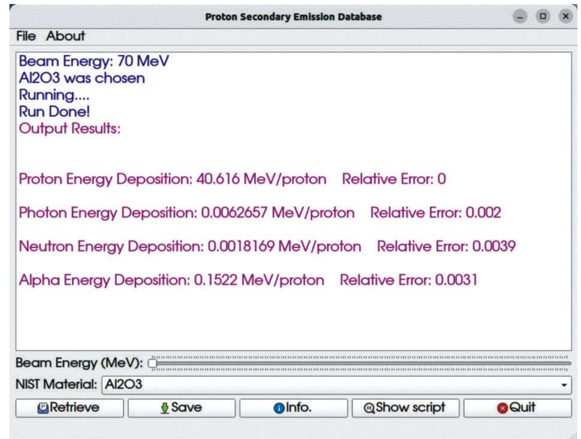

Figure 2. ProtonSED GUI program illustrating energy deposition by primary and secondary particles resulting from 70 MeV proton irradiation of an Al_2O_3 target

Correlation matrices for proton, photon, neutron, and alpha particle energy deposition in the present database were calculated. The Pearson correlation coefficient r between two variables x and y was defined as

$$r_{xy} = \frac{\sum_{i=1}^{n}(x_i-\bar{x})(y_i-\bar{y})}{\sqrt{\sum_{i=1}^{n}(x_i-\bar{x})^2}\sqrt{\sum_{i=1}^{n}(y_i-\bar{y})^2}} \qquad (1)$$

where x_i and y_i are individual sample values of variables x and y, and $\bar{x}$ and $\bar{y}$ are the means of x and y.

This quantifies the strength and direction of the linear relationship between two variables. The results were obtained for proton-photon, proton-neutron, and proton-alpha combinations. The correlation matrices for liquid water, skeletal muscle, air, and CO_2 were shown in the present work.

The computations were performed on the GNU/Linux computer with dual Xeon E5-2630 2.40 GHz CPUs and coupled wsith PHITS version 3.28. The Intra-Nuclear Cascade Liege (INCL) model was used to explain the nuclear reaction involved in the present work. The INCL model was adopted as the default for simulating nuclear reactions induced by pro-

Table 2. Aset of selected elements and compounds for verification and validation of our model

Proton energy [MeV]	Compound	Proton energy [MeV]	Element
70	Tissue equivalent plastic	70	Carbon (C)
100	Air	100	Nitrogen (N)
120	CO_2	120	Oxygen (O)
150	Mylar	150	Silicon (Si)
200	SiO_2	200	Molybdenum (Mo)
220	NaI	220	Lead (Pb)
250	Water, liquid	250	Uranium (U)

tons. The stopping powers for charged particles and nuclei were calculated using the ATIMA code [27] implemented in the PHITS MC package. In general, PHITS automatically calculates the stopping power of each material using the ATIMA model. The ENDF70PROT, MCPLIB84, and ENDF71x databases were used in the MCNP6.2 computations.

RESULTS AND DISCUSSION

Benchmarking with MCNP6.2

The comparison of the results from our ProtonSED program, based on the PHITS MC package, with the MCNP6.2 MC package for selected compounds and elements, is shown in figs. 3 and 4, respectively. Energy deposition results from protons and secondary particles obtained with ProtonSED and MCNP6.2 are in close agreement.

In addition to the energy deposition results, the average relative error associated with the MC computations using ProtonSED and MCNP6.2 was obtained and is presented in fig. 5. The relative errors were averaged for the compounds and elements shown in figs. 3 and 4, respectively. The average relative error values were found to be less than ~8 %, indicating that the obtained results are statistically reliable for incident protons and secondary particles. The average relative error values presented in fig. 5 were calculated by taking the arithmetic mean of the relative errors for the compounds and elements shown in figs. 3 and 4, respectively. For these materials, the production of secondary particles is less probable,

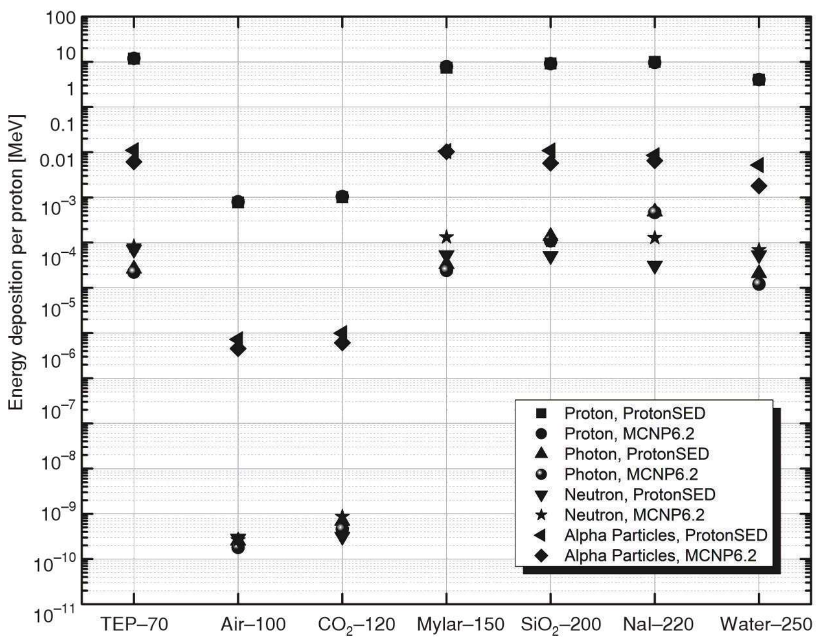

Figure 3. Comparison of energy deposition results between ProtonSED and MCNP6.2 for selected compounds at different incident proton energies, validating the present platform against the well-established MCNP package

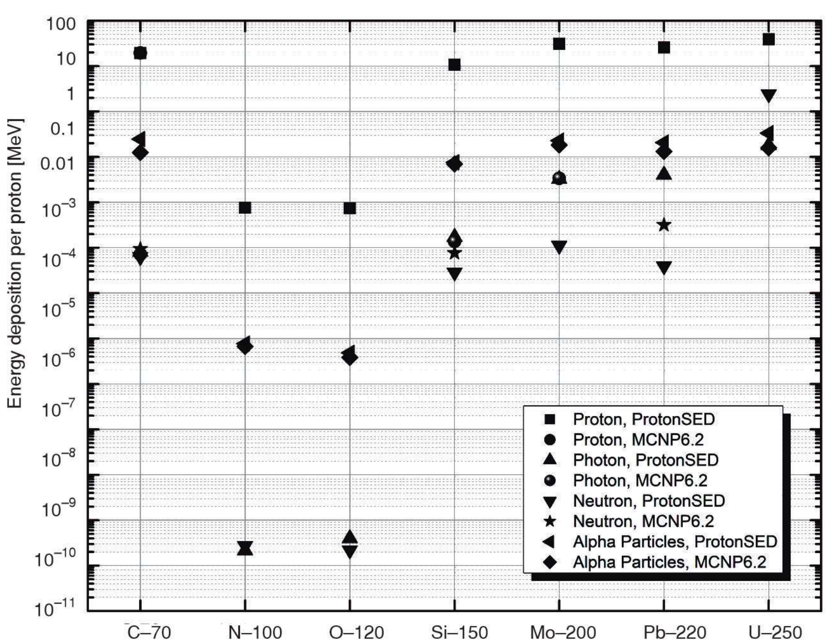

Figure 4. Comparison of energy deposition results between ProtonSED and MCNP6.2 for selected elements at different incident proton energies, validating the present platform against the well-established MCNP package

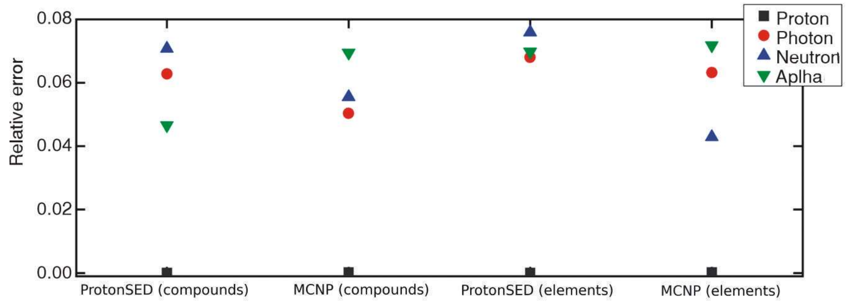

Figure 5. Comparison of the average relative errors associated with statistical uncertainties obtained with ProtonSED and MCNP6.2

which contributes to a relatively smaller impact. Consequently, the maximum average relative error observed was ~8 %, which is acceptable. We recommend that readers refer to the individual relative error values reported by our program for each specific case, as these provide a more accurate and case-specific measure of statistical uncertainty.

Energy deposition from incident protons and secondary particles

To demonstrate the capabilities of the present model, we have selected 8 compounds namely, adipose tissue, Al_2O_3, bone equivalent plastic, air equivalent plastic, cellulose nitrate, ethzlene, lithium tetraborate, skeletal muscle. For each compound, three different incident proton energies in the range of 70 MeV to 250 MeV were considered. The energy deposition of protons, photons, neutrons, and alpha particles (in MeV per proton) was determined using the current program. The results obtained, together with the associated relative errors, are presented in tab. 3. These results were further validated through manual execution of the generated scripts using the PHITS MC package, and no inconsistencies were observed. The reported low relative error values are desirable, mainly as they ensure the accuracy and reliability of the results. Considering that liquid water and adipose tissue are in the interest of radiation dosimetry, the variation of energy deposition from primary protons and secondary photons, neutrons and alpha particles on different incident proton energies were obtained and shown in fig. 6. The results indicate that proton energy deposition decreases with increasing incident pro-

Table 3. The results obtained for eight different selected compounds at three distinct incident proton beam energies as provided by the ProtonSED program

Material	Energy [MeV]	Proton		Photon		Neutron		Alpha	
		Deposition	Rel. error	Deposition	Rel. error	Deposition	Rel. error	Deposition	Rel. error
Adipose tissue	70	9.70	0.00	$1.91\cdot10^{-4}$	$5.70\cdot10^{-3}$	$5.20\cdot10^{-4}$	$7.10\cdot10^{-3}$	$7.89\cdot10^{-2}$	$5.20\cdot10^{-3}$
Adipose tissue	160	5.07	$1.00\cdot10^{-4}$	$1.33\cdot10^{-4}$	$6.70\cdot10^{-3}$	$4.24\cdot10^{-4}$	$8.20\cdot10^{-3}$	$6.66\cdot10^{-2}$	$5.80\cdot10^{-3}$
Adipose tissue	250	3.80	$1.00\cdot10^{-4}$	$1.33\cdot10^{-4}$	$8.10\cdot10^{-3}$	$4.50\cdot10^{-4}$	$8.20\cdot10^{-3}$	$6.81\cdot10^{-2}$	$5.80\cdot10^{-3}$
Al_2O_3	70	$4.06\cdot10^{1}$	0.00	$6.27\cdot10^{-3}$	$2.00\cdot10^{-3}$	$1.82\cdot10^{-3}$	$3.90\cdot10^{-3}$	$1.52\cdot10^{-1}$	$3.10\cdot10^{-3}$
Al_2O_3	160	$1.82\cdot10^{1}$	$1.00\cdot10^{-4}$	$4.10\cdot10^{-3}$	$2.50\cdot10^{-3}$	$1.51\cdot10^{-3}$	$4.40\cdot10^{-3}$	$1.72\cdot10^{-1}$	$3.80\cdot10^{-3}$
Al_2O_3	250	$1.36\cdot10^{1}$	$1.00\cdot10^{-4}$	$4.04\cdot10^{-3}$	$3.10\cdot10^{-3}$	$1.63\cdot10^{-3}$	$4.30\cdot10^{-3}$	$2.06\cdot10^{-1}$	$3.70\cdot10^{-3}$
Bone eq. plastic	70	$1.43\cdot10^{1}$	0.00	$5.28\cdot10^{-4}$	$4.20\cdot10^{-3}$	$9.06\cdot10^{-4}$	$5.30\cdot10^{-3}$	$1.14\cdot10^{-1}$	$4.20\cdot10^{-3}$
Bone eq. plastic	160	7.35	$1.00\cdot10^{-4}$	$3.82\cdot10^{-4}$	$5.00\cdot10^{-3}$	$7.74\cdot10^{-4}$	$6.10\cdot10^{-3}$	$1.01\cdot10^{-1}$	$4.80\cdot10^{-3}$
Bone eq. plastic	250	5.51	$1.00\cdot10^{-4}$	$3.89\cdot10^{-4}$	$6.60\cdot10^{-3}$	$8.27\cdot10^{-4}$	$6.10\cdot10^{-3}$	$1.04\cdot10^{-1}$	$4.90\cdot10^{-3}$
Air eq. plastic	70	$1.64\cdot10^{1}$	0.00	$7.73\cdot10^{-4}$	$3.60\cdot10^{-3}$	$8.78\cdot10^{-4}$	$4.40\cdot10^{-3}$	$1.49\cdot10^{-1}$	$3.60\cdot10^{-3}$
Air eq. plastic	160	8.40	$1.00\cdot10^{-4}$	$5.39\cdot10^{-4}$	$4.30\cdot10^{-3}$	$7.20\cdot10^{-4}$	$5.20\cdot10^{-3}$	$1.35\cdot10^{-1}$	$4.30\cdot10^{-3}$
Air eq. plastic	250	6.29	$1.00\cdot10^{-4}$	$5.42\cdot10^{-4}$	$5.90\cdot10^{-3}$	$7.54\cdot10^{-4}$	$5.20\cdot10^{-3}$	$1.40\cdot10^{-1}$	$4.30\cdot10^{-3}$
Cellulose nitrate	70	$1.43\cdot10^{1}$	0.00	$6.23\cdot10^{-4}$	$3.80\cdot10^{-3}$	$6.78\cdot10^{-4}$	$5.70\cdot10^{-3}$	$9.95\cdot10^{-2}$	$4.50\cdot10^{-3}$
Cellulose nitrate	160	7.37	$1.00\cdot10^{-4}$	$4.19\cdot10^{-4}$	$4.60\cdot10^{-3}$	$5.33\cdot10^{-4}$	$6.50\cdot10^{-3}$	$9.62\cdot10^{-2}$	$4.90\cdot10^{-3}$
Cellulose nitrate	250	5.53	$1.00\cdot10^{-4}$	$4.09\cdot10^{-4}$	$5.80\cdot10^{-3}$	$5.61\cdot10^{-4}$	$6.40\cdot10^{-3}$	$1.04\cdot10^{-1}$	$4.80\cdot10^{-3}$
Ethylene	70	$1.23\cdot10^{-2}$	0.00	$3.18\cdot10^{-10}$	$1.61\cdot10^{-1}$	$8.10\cdot10^{-10}$	$2.24\cdot10^{-1}$	$1.10\cdot10^{-5}$	$1.29\cdot10^{-1}$
Ethylene	160	$6.67\cdot10^{-3}$	0.00	$2.53\cdot10^{-10}$	$2.04\cdot10^{-1}$	$9.78\cdot10^{-10}$	$2.11\cdot10^{-1}$	$8.66\cdot10^{-6}$	$1.53\cdot10^{-1}$
Ethylene	250	$4.99\cdot10^{-3}$	0.00	$1.34\cdot10^{-10}$	$2.55\cdot10^{-1}$	$8.61\cdot10^{-10}$	$2.46\cdot10^{-1}$	$8.25\cdot10^{-6}$	$1.40\cdot10^{-1}$
Lithium-tetraborate	70	$2.32\cdot10^{1}$	0.00	$1.54\cdot10^{-3}$	$3.00\cdot10^{-3}$	$1.42\cdot10^{-3}$	$4.40\cdot10^{-3}$	$1.66\cdot10^{-1}$	$3.20\cdot10^{-3}$
Lithium-tetraborate	160	$1.15\cdot10^{1}$	$1.00\cdot10^{-4}$	$9.88\cdot10^{-4}$	$3.70\cdot10^{-3}$	$1.11\cdot10^{-3}$	$5.10\cdot10^{-3}$	$1.58\cdot10^{-1}$	$3.70\cdot10^{-3}$
Lithium-tetraborate	250	8.59	$1.00\cdot10^{-4}$	$9.70\cdot10^{-4}$	$5.00\cdot10^{-3}$	$1.14\cdot10^{-3}$	$5.10\cdot10^{-3}$	$1.71\cdot10^{-1}$	$3.70\cdot10^{-3}$
Muscle, skeletal	70	$1.07\cdot10^{1}$	0.00	$3.28\cdot10^{-4}$	$4.60\cdot10^{-3}$	$6.27\cdot10^{-4}$	$6.60\cdot10^{-3}$	$5.09\cdot10^{-2}$	$6.20\cdot10^{-3}$
Muscle, skeletal	160	5.57	$1.00\cdot10^{-4}$	$2.23\cdot10^{-4}$	$5.50\cdot10^{-3}$	$5.09\cdot10^{-4}$	$7.50\cdot10^{-3}$	$5.35\cdot10^{-2}$	$6.60\cdot10^{-3}$
Muscle, skeletal	250	4.17	$1.00\cdot10^{-4}$	$2.17\cdot10^{-4}$	$6.50\cdot10^{-3}$	$5.39\cdot10^{-4}$	$7.50\cdot10^{-3}$	$5.92\cdot10^{-2}$	$6.40\cdot10^{-3}$

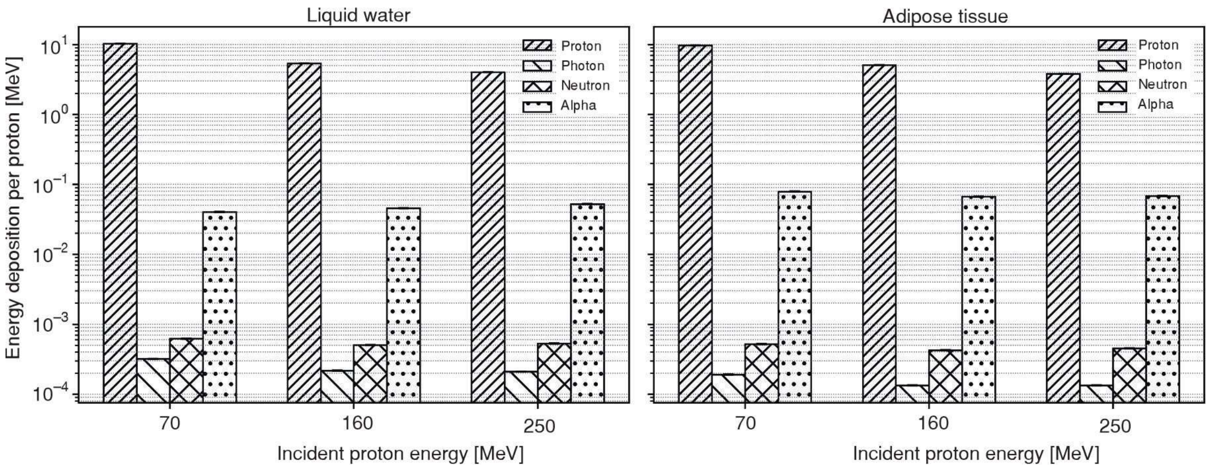

Figure 6. Comparison between liquid water and adipose tissue energy depositions from primary and secondary particles upon exposure to 70 MeV, 160 MeV, and 250 MeV incident protons obtained from our database

ton energies, primarily due to fewer Coulomb interactions at higher incident proton energies. Moreover, proton energy deposition dominates in both media by several orders of magnitude compared to that of secondary particles. The yields of secondary particles follow the same monotonic decline with the incident proton energy, mainly because the nuclear inelastic cross sections for (p, n) and (p, γ) reactions decrease beyond ~100 MeV. At higher energies, protons also deposit a larger fraction of their energy outside the small 1 cm^3 scoring volume before nuclear reactions occur. Unlike neutrons and photons, alpha particle energy deposition is consistently higher in adipose and even increases slightly with energy in both media, which is attributed primarily to (p, α) nuclear reactions on light nuclei.

Correlation of energy deposition between protons and secondary particles

The correlation matrices for energy deposition in different materials reveal varying interaction patterns based on material composition and density, as shown in fig. 7. In liquid water and skeletal muscle, there is a strong positive correlation between proton, photon, and neutron energy depositions, with values ranging from 0.8 to 0.98. This indicates that these radiation types interact in a similar manner within these materials, with dosimetric properties that show close agreement. Both materials also exhibit a strong negative correlation between proton and alpha energy depositions, approximately –0.93 in liquid water and –0.89 in skeletal muscle, suggesting that an increase in proton dose corresponds to a decrease in alpha dose. This behavior is primarily attributed to the changes in the energy of the generated alpha particles at different incident proton energies.

In contrast, air and CO_2 display different patterns. In air, the correlations are generally lower, with proton-photon correlation of 0.75 being the highest. This indicates that radiation interactions and subsequent energy deposition in gaseous media are less coupled. The CO_2 shows moderate correlations across different secondary particle types, with proton-photon at 0.88 and proton-alpha at 0.81, indicating some level of interdependence but not as strong as those in denser materials (*i.e.*, liquid water and skeletal muscle). These differences highlight that denser materials, such as liquid water and skeletal muscle, tend to have more consistent energy depositions and coupling among different secondary radiation types. By comparison, gases, such as air and CO_2, show weaker and more variable correlations due to differences in energy deposition and scattering properties. Secondary particle production is less frequent in gases because the lower atomic density leads to fewer nuclear reactions. However, high-energy protons can still produce secondary particles upon interaction with individual gas molecules, such as ionized particles or gamma radiation. Therefore, weaker correlations are observed compared to materials of relatively higher atomic density.

The use of a correlation matrix for comparing energy depositions of primary protons and secondary particles, such as photons, neutrons, and alpha particles, provides significant advantages in evaluating and understanding the dosimetric properties of different materials. These advantages can be achieved by analyzing the correlations between these energy depositions. Considering this, strong positive correlations between incident proton and dose from secondary particles might indicate that these particles exhibit similar energy deposition characteristics in a particular material, which could be important in applications where dose consistency across particle types is desired. Additionally, this approach enables a quantitative comparison of how various materials respond to radiation, as correlation patterns can reveal unique interaction profiles, making them suitable for different applications such as radiation shielding or therapy.

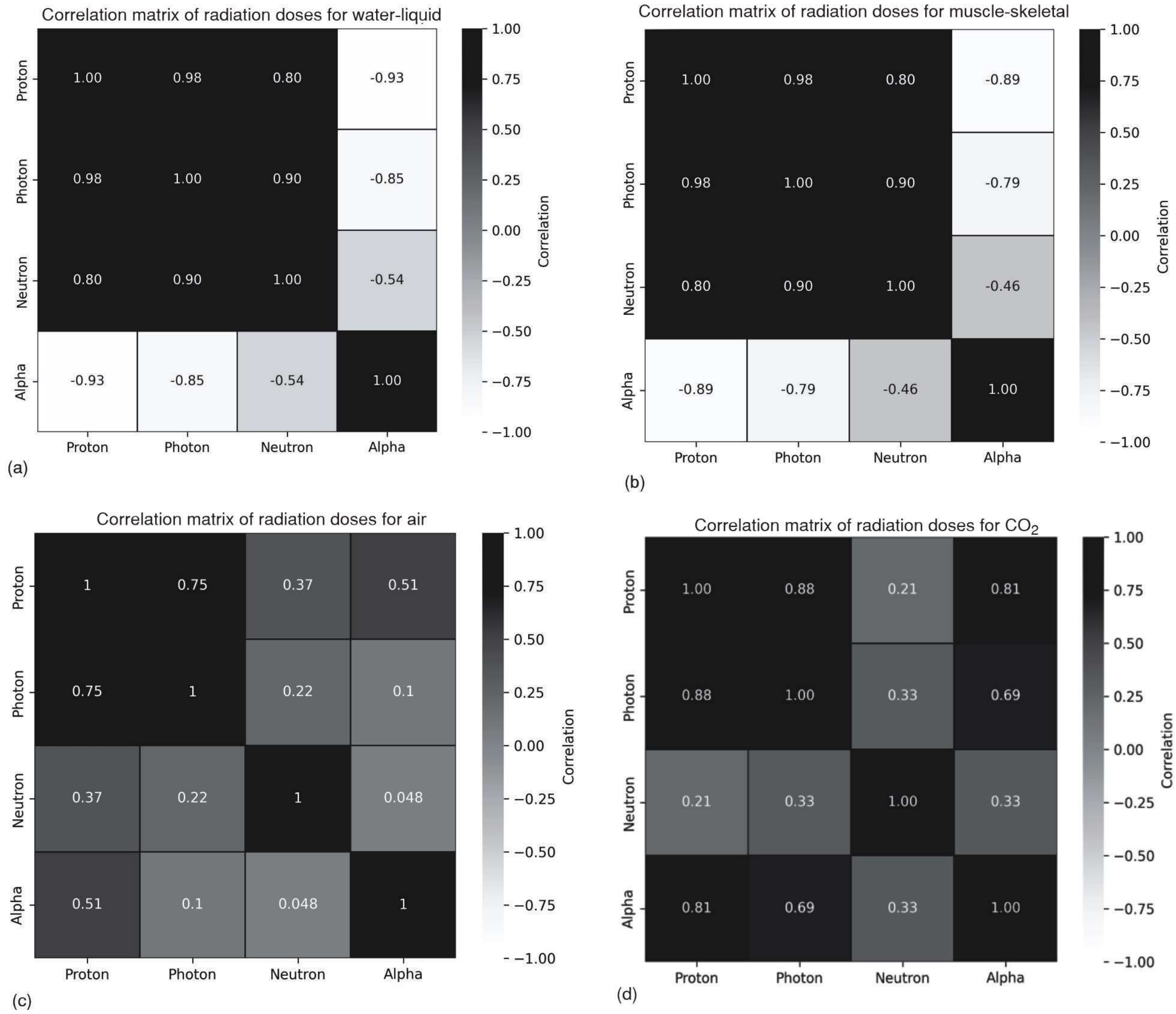

Figure 7. Correlation matrix of MC simulated energy deposition events between incident primary protons and secondary particles in four representative media: (a) liquid water, (b) skeletal muscle, (c) air, and (d) CO_2 highlighting how each secondary species (photons, neutrons, and alpha particles) contributes to, or diverges from, the proton energy deposition within each material

INTERACTIVE PHITS MODEL

The current model represents a unit-volume cylinder, which closely resembles the geometry and sensitive volume of widely used ionization chambers in radiation dosimetry experiments. This 1 cm^3 volume provides a reliable approximation of local energy deposition and captures key features related to the energy deposition of both primary and secondary particles. However, given the vast variety of potential geometries and dimensions that users may require, it is important to account for the flexibility and diverse needs in modeling. To address this, we have developed a separate, interactive GUI model hosted on a web server named interactive PHITS (iPHITS) [28] (stands for interactive PHITS). This tool allows users to model a variety of geometries, including rectangular parallelepipeds, cylinders, and spheres. Additionally, users can easily set key parameters such as beam energy, direction, radius, and other essential MC parameters through a user-friendly and interactive interface.

SUMMARY AND CONCLUSIONS

The ProtonSED program, coupled with the well-established PHITS MC package, accurately calculates the energy deposition of the incident proton beam and secondary particles (*i.e.*, neutrons, photons and alpha particles) produced through interactions between the proton beam and the target. The target materials (*i. e*., compounds and elements) were obtained from the NIST database. Several results have been compared for validation and verification with the MCNP6.2 package, showing a good agreement and low statistical uncertainties. The ProtonSED program is an accurate and reliable tool for researchers working with proton beams in the medical physics energy range. The present database and program enable users to estimate the absorbed dose from primary protons and secondary neutrons, photons, and alpha particles without the need for complex MC computations. Future work will focus on extending this database to incorporate other physical quantities, including primary and secondary particle fluence as well as the energy distribution of the proton-induced secondary particles. Additionally, expanding the material coverage of the present database would benefit a broader range of researchers.

ACKNOWLEDGEMENT

This work was supported by the Japan Society for the Promotion of Science (JSPS) through JSPS KAKENHI (Grant No. 21F21103) and JSPS (Grant No. JPJSBP120218804), and by the City University of Hong Kong (Research Grant Nos. 9229151 and 9220124).

AUTHORS' CONTRIBUTIONS

N. Safakatti Karakoc: conceptualization, methodology, software, data curation, visualization, writing-original draft. H. Watabe: conceptualization; supervision; project administration; funding acquisition; writing-review & editing. P. K. N. Yu: conceptualization; methodology; resources; supervision; writing-review & editing. D. Ž. Krstić: methodology; validation; investigation; writing-review & editing. D. R. Nikezić: methodology; validation; investigation; writing-review & editing. Z. M. Jovanović: software; investigation; data curation; writing-review & editing. A. K. F. Haque: validation; resources; writing-review & editing. R. Islam: formal analysis; validation; visualization; writing-review & editing. M. Shahmohammadi Beni: Conceptualization; methodology; software; formal analysis; visualization; writing-original draft; supervision; project administration.

DATA AVAILABILITY

All data, executables, and source code files can be downloaded from: https://figshare.com/articles/software/A_dosimetric_proton-induced_secondary_particle_emission_database_for_NIST_elements_and_compounds/24056985.

REFERENCES

[1] Mitin, T., Zietman, A. L., Promise and Pitfalls of Heavy Particle Therapy, *Journal of Clinical Oncology, 32* (2014), 2855
[2] Safavi, A. H., *et al*., Proton Therapy in Canada: Toward Universal Access and Health Equity with a Publicly Funded Facility, *International Journal of Radiation Oncology*, Biology, *Physics, 116* (2023), 2, pp. 394-403
[3] Nogueira, L. M., *et al*., Assessment of Proton Beam Therapy Use Among Patients with Newly Diagnosed Cancer in the US, 2004-2018, *JAMA Network Open, 5* (2022), e229025
[4] Mohan, R., A Review of Proton Therapy – Current Status and Future Directions, *Precision Radiation Oncology, 6* (2022), 2, pp. 164-176
[5] Paganetti, H., Nuclear Interactions in Proton Therapy: Dose and Relative Biological Effect Distributions Originating from Primary and Secondary Particles, *Physics in Medicine & Biology, 47* (2002), 747
[6] Luo, C., *et al*., Study on Occupational Exposure of Medical Staff Caused by Induced Radioactivity in the Treatment Room of Medical Heavy-Ion Facility, *Nucl Technol Radiat, 38* (2023), 1, pp. 39-47
[7] Tang, X. Q., *et al*., Simulation and Measurement of X-Ray Scattered Radiation in Radiodiagnosis, *Nucl Technol Radiat, 38* (2023), 2, pp. 125-134
[8] Pham, H. L., *et al*., Photon Beam Modeling: A Comparative Study of PRIMO and GATE Simulation Toolkits for the TrueBeam STx linac, *Nucl Technol Radiat, 39* (2024), 1, pp. 58-65
[9] Duo, W., *et al*., Monte Carlo Simulation-Based Dosimetric Evaluation of a Novel ^{125}I Brachytherapy source: Comparative Assessment of Dosimetry Parameters and Shadowing Effects, *Nucl Technol Radiat, 39* (2024), 4, pp. 312-317
[10] Jiang, H., *et al*., Simulation of Organ Specific Patient Effective Dose Due to Secondary Neutrons in Proton Radiation Treatment, *Physics in Medicine & Biology, 50* (2005), 4337
[11] Howell, R. M., Burgett, E. A., Secondary Neutron Spectrum from 250 MeV Passively Scattered Proton Therapy: Measurement with an Extended Range Bonner Sphere System, *Medical Physics, 41* (2014), 092104
[12] Athar, B. S., Paganetti, H., Neutron Equivalent Doses and Associated Lifetime Cancer Incidence Risks for Head & Neck and Spinal Proton Therapy, *Physics in Medicine & Biology, 54* (2009), 4907
[13] Jarlskog, C. Z., Paganetti, H., Risk of Developing Second Cancer from Neutron Dose in Proton Therapy as Function of Field Characteristics, Organ, and Patient Age, *International Journal of Radiation Oncology, Biology, Physics, 72* (2008), 1, pp. 228-235
[14] ***, Monte Carlo N-Particle (MCNP) Package, Los Alamos National Laboratory, Los Alamos, New Mexico, USA, n.d., https://mcnp.lanl.gov/
[15] ***, GEANT4 Monte Carlo Package, European Organization for Nuclear Research (CERN), Geneva, Switzerland, n.d., https://geant4.web.cern.ch
[16] ***, FLUKA Monte Carlo Package, FLUKA Website, n.d., http://www.fluka.org/fluka.php
[17] ***, PHITS Monte Carlo Package, Japan Atomic Energy Agency (JAEA), Tokai, Ibaraki, Japan, n.d., https://phits.jaea.go.jp/
[18] Cliffe, K. A., *et al*., Multilevel Monte Carlo Methods and Applications to Elliptic PDE with Random Coefficients, *Computing and Visualization in Science, 14* (2011), 1, pp. 3-15
[19] Fan, J., *et al*., A Practical Monte Carlo MU Verification Tool for IMRT Quality Assurance, *Physics in Medicine & Biology, 51* (2006), 2503
[20] Shan, J., *et al*., Virtual Particle Monte Carlo: A New Concept to Avoid Simulating Secondary Particles in Proton Therapy Dose Calculation, *Medical Physics, 49* (2022), 10, pp. 6666-6683
[21] Ekinci, F., *et al*., Monte Carlo Simulation of TRIM Algorithm in Ceramic Biomaterial in Proton Therapy, *Materials, 16* (2023), 4833
[22] ***, National Institute of Standards and Technology (NIST), ASTAR and PSTAR Materials, n.d., https://physics.nist.gov/cgi-bin/Star/compos.pl?ap
[23] Shahmohammadi Beni, M., *et al*., Development of PHITS Graphical User Interface for Simulation of Positron Emitting Radioisotopes Production in Common Biological Materials During Proton Therapy, *Journal of Radiation Research, 63* (2022), 3, pp. 385-392
[24] Yu, K. N., *et al*., Shahmohammadi Beni, M., DynamicMC: An Open Source GUI Program Coupled with

MCNP for Modeling Relative Dynamic Movement of Radioactive Source and ORNL Phantom in a 3-Dimensional Radiation Field, *Health Physics, 124* (2023), 4, pp. 301-309

[25] Watabe, H., *et al*., Development of an Open Source GUI Computer Program for Modelling Irradiation of Multi Segmented Phantoms Using Grid-Based System for PHITS, *Nuclear Engineering and Technology, 55* (2023), 1, pp. 373-377

[26] Watabe, H., *et al*., Development of DynamicMC for PHITS 12 Monte Carlo package, *Radiation Protection Dosimetry, 200* (2024), 2, pp. 130-142

[27] ***, ATIMA Code, GSI Helmholtzzentrum für Schwerionenforschung, n.d., https://web-docs.gsi.de/~weick/atima/

[28] ***, iPHITS program website, n.d., https://msbcyrictohoku.github.io/iPHITS/

Received on September 10, 2025
Accepted on November 11, 2025

Нурсел САФАКАТИ КАРАКОЧ, Хироши ВАТАБЕ, Петер Кван Нгок ЈУ, Драгана Ж. КРСТИЋ, Драгослав Р. НИКЕЗИЋ, Зоран М. ЈОВАНОВИЋ, Абул Калам Фазул ХАКЕ, Рафикул ИСЛАМ, Мехрдад ШАХМОХАМАДИ БЕНИ

ДОЗИМЕТРИЈСКА БАЗА ПОДАТАКА И ПРОУЧАВАЊЕ КОРЕЛАЦИЈЕ ПРОТОНИМА ИНДУКОВАНИХ СЕКУНДАРНИХ ЧЕСТИЦА

Као одговор на велику потражњу за протонском терапијом као методом лечења рака последњих година, спроведене су свеобухватне студије за прецизно израчунавање дозе. Међутим, секундарне честице настале током протонског зрачења у енергетском опсегу од 70-250 MeV представљају изазове, као што су потенцијална оштећења повезана са зрачењем на материјалима који нису циљани. Да бисмо размотрили ове проблеме, развили смо базу података отвореног кода и рачунарски програм под називом База података о секундарној емисији индукованој протонима (ProtonSED). Садашња база података укључује једињења и елементе Националног института за стандарде и технологију (NIST) у цилиндру јединичне запремине, како би се одредили примарни протони и секундарне честице као што су неутрони, фотони и алфа честице. Такође су одређене матрице корелације за таложење енергије из примарних протона и секундарних честица. Садашња база података и приступ са матрицом корелације биће корисни код зрачења која укључују протонске снопове високе енергије.

Кључне речи: програм за транспорт честица и тешких јона (PHITS), Монте Карло метода, протонска терапија, база података о секундарној емисији